Available online at www.sciencedirect.com
SCIENCE DIRECT®
Inorganica Chimica Acta 358 (2005) 2403–2412
Inorganica Chimica Acta
www.elsevier.com/locate/ica

Complexes of Cu^{II} with mixed-donor phenanthroline-containing macrocycles: analysis of their structural, redox and spectral properties in the context of Type-1 blue copper proteins biomimetic models

Massimiliano Arca [a], Gholamhassan Azimi [b], Francesco Demartin [c], Francesco A. Devillanova [a], Lluis Escriche [d], Alessandra Garau [a], Francesco Isaia [a], Raikko Kivekas [e], Vito Lippolis [a,*], Vicent Muns [d], Alessandro Perra [a], Mojtaba Shamsipur [f], Luigi Sportelli [g], Abdollah Yari [f]

[a] *Dipartimento di Chimica Inorganica ed Analitica, Università degli Studi di Cagliari, S.S. 554 Bivio per Sestu, 09042 Monserrato, Cagliari, Italy*
[b] *Department of Chemistry, Arak University, Shariati sp., Arak, Iran*
[c] *Dipartimento di Chimica Strutturale e Stereochimica Inorganica, Università di Milano, Via G. Venezian 21, 20133 Milano, Italy*
[d] *Departement de Química (Unit Inorganica), Universitat Autònoma de Barcelona, 08193 Bellaterra, Barcelona, Spain*
[e] *Department of Chemistry, University of Helsinky, P.O. Box 55, FIN 00014 Helsinky, Finland*
[f] *Department of Chemistry, Razi University, Kermanshah, Iran*
[g] *Laboratorio di Biofisica Molecolare, Dipartimento di Fisica and Unità INFM, Università della Calabria, 87036 Rende, Cosenza, Italy*

Received 20 December 2004; accepted 21 January 2005

Abstract

The macrocycles L^1–L^3 having N_2S_2O-, N_2S_2-, and N_2S_3-donor sets, respectively, and incorporating the 1,10-phenanthroline unit interact in EtOH and MeCN solutions with Cu^{II} to give 1:1 $[M(L)]^{2+}$ complex species. The compounds $[Cu(L^1)(ClO_4)]ClO_4$ (**1**), $[Cu(L^2)(ClO_4)]ClO_4 \cdot \frac{1}{2}H_2O$ (**2**) and $[Cu(L^3)](ClO_4)_2$ (**3**) were isolated at the solid state and the first two also characterised by X-ray diffraction studies. The conformation adopted by L^1 and L^2 in the cation complexes reveals the aliphatic portion of the rings folded over the plane containing the heteroaromatic moiety with the ligands encapsulating the metal centre within their cavity by imposing, respectively, a square-based pyramidal and a square planar geometry. In both complexes, the metal ion completes its coordination sphere by interacting with a ClO_4^- ligand. The compound $[Cu(L^3)_2](PF_6)_2$ (**4**) containing a 1:2 cation complex was also isolated at the solid state: EPR spectroscopy measurements suggest the presence of a CuN_4 chromophore in this complex. The EPR and electronic spectral features of **1**–**4** have been studied and their redox properties examined in comparison with those observed for Type-1 blue copper proteins.

The reactivity of L^1–L^3 has also been tested toward stoichiometric amounts of the Cu^I salt $[CuCl(PPh_3)_3]$.

Keywords: Macrocycles; Phenanthroline; Type-1 blue copper proteins; X-ray diffraction

1. Introduction

The spectral and redox properties of Type-1 blue copper proteins [1–6] are strongly determined by the particular chemical environment at the metal centre in the

* Corresponding author. Tel.: +39 070 675 4467; fax: +39 070 675 4456.
E-mail address: lippolis@unica.it (V. Lippolis).

0020-1693/$ - see front matter © 2005 Elsevier B.V. All rights reserved.
doi:10.1016/j.ica.2005.01.014

active site, which in general comprises two N- (from histidine residues) and two S-donors (from a cysteine and a methionine residue) arranged in a distorted tetrahedral geometry [1–6]. In azurin, one oxygen atom from a glycine residue is also strongly coordinated to Cu^{II} to give a distorted trigonal bipyramidal coordination geometry [5].

Many Cu^{II} complexes have been synthesised over several decades with the aim of reproducing Type-1 coordination geometry and addressing the structure/spectral and redox properties relationship [7–9]. In this respect, macrocyclic ligands incorporating N/S/O donors have been used extensively to model the active sites of blue copper proteins [10–16] due to their restricted framework conformability, which can be considered responsible for unusual constrained coordination geometries at the metal centre, and consequently for peculiar electronic spectra and redox potentials of the resulting complexes.

For example, copper(II) complexes of macrocyclic ligands, such as [14]ane$S_xN_{(4-x)}$ ($x = 1$–4), have been extensively studied [13,14,16]; substitution of a thioether for an amine donor leads to an increase in $E_{1/2}$ for the Cu^{II}/Cu^{I} couple and parallely to a shift in the absorption spectrum to longer wavelengths and higher absorption coefficients. In some cases, the spectroscopic and redox properties of Cu^{II} complexes of these ligands are similar to those of Type-1 native blue copper proteins, though the coordination geometry around Cu^{II} tends to be square-based. Macrocyclic ligands with restricted flexibility have also been synthesised by introducing aromatic moieties in the cyclic structure with the aim of having Cu^{II} and Cu^{I} complexes with identical donor sets and closely related geometries [14]. Addison and co-workers [15] have reported closely related pairs of Cu^{II} and Cu^{I} complexes with Schiff-base macrocycles derived from the condensation of 1,4-bis(2-formylphenyl)-1,4-dithiabutane and aliphatic α,ω-diamine; on changing the length of the N–N linkage a tetrahedral environment can be provided to Cu^{I}, thus making the reduction potential for the Cu^{II}/Cu^{I} couple more positive.

Recently, we have reported the synthesis and coordinating properties towards some d^8 and d^{10} transition metal ions of the mixed aza-thioether crowns L^1–L^3 incorporating the 1,10-phenanthroline sub-unit [17–21]. These ligands have shown peculiar chelating properties strongly determined by conformational constraints imposed by the phenanthroline unit on the rest of the aliphatic chain of the ring. Now, we have investigated the coordination chemistry of L^1, L^2, and L^3 towards Cu^{II}. The effect of the phenanthroline unit on the spectral and redox properties of the resulting complexes has also been analysed in the context of Type-1 blue copper protein biomimetic models.

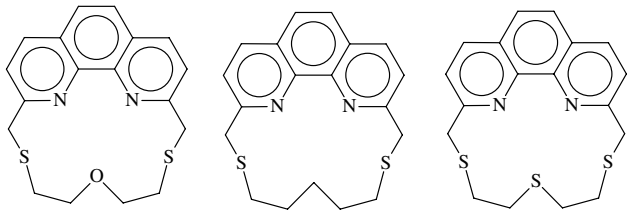

L^1 L^2 L^3

2. Experimental

All melting points are uncorrected. Microanalytical data were obtained using a Fisons EA CHNS-O instrument ($T = 1000$ °C). FAB mass spectra (3-NOBA matrix) were recorded at the Institut für Organische Chemie der Technischen Universität, Braunschweig. The ^1H and ^{13}C NMR spectra were recorded on a Varian VXR300 spectrometer (operating at 75.4 MHz). The spectrophotometric measurements were carried out using a Cecil 9000 spectrophotometer.

Electron paramagnetic resonance (EPR) measurements were carried out using a Bruker Mod. ER 200D SRC X-band spectrometer equipped with the TE_{102} standard cavity and the ESP 1600 Data System. Cyclic voltammetry was performed using a conventional three-electrode cell, with a platinum double-bead electrode and Ag/AgCl reference electrode (in 3.5 M KCl; 0.2050 V vs SHE). All measurements were taken in a 0.1 M MeCN solution of Bu_4NBF_4. A stream of argon was passed through the solution prior to the scan. Data were recorded on a computer-controlled EG&G (Princeton Applied Research) potentiostat-galvanostat Model 273 EG&G, using model 270 electrochemical analysis software.

Reagent grade copper perchlorate, copper chloride dihydrate, acetonitrile (MeCN), and ethanol (EtOH) (all from Aldrich) were of the highest purity available and used without any further purification. The salt $[CuCl(PPh_3)_3]$ was synthesised according to the literature [22]. The ligands L^1, L^2 and L^3 were synthesised as previously reported [17–21].

Caution! Perchlorate salts are potentially explosive; these compounds must be handled with great care.

*2.1. Synthesis of $[Cu(L^1)(ClO_4)]ClO_4$ (**1**), $[Cu(L^2)(ClO_4)]ClO_4 \cdot \frac{1}{2}H_2O$ (**2**) and $[Cu(L^3)](ClO_4)_2$ (**3**)*

Addition of one equivalent of $Cu(ClO_4)_2 \cdot 2H_2O$ in EtOH (5 ml) to a solution of L^1–L^3 (10^{-3} mol) in EtOH–CH_2Cl_2 (10 ml, 2:1 v/v ratio) maintained at room temperature under N_2 afforded blue-green (**1**), light blue (**2**), and purple (**3**) solids after four hours stirring.

1: Re-crystallisation of the crude product by slow diffusion of Et_2O into a MeCN solution gave $[Cu(L^1)(ClO_4)]ClO_4$ (51% yield) as well shaped blue prisms: m.p. 260 °C with decomposition. Elemental Analysis: *Anal.* Calc. for $C_{18}H_{18}Cl_2CuN_2O_9S_2$: C, 35.7; H, 3.0; N, 4.6; S, 10.6. Found: C, 36.1; H, 3.1; N, 4.6; S, 10.6%. FAB mass spectrum (3-noba matrix): *m/z* 504, 405; calc. for $[^{63}Cu(L^1)(ClO_4)]^+$ and $[^{63}Cu(L^1)]^+$ 504 and 405, respectively. Electronic spectrum (MeCN): $\lambda_{max} = 230$ ($\varepsilon_{max} = 48\,000$), 278 (29 600), 361 (4400), 639 nm (400 M^{-1} cm^{-1}).

2: Re-crystallisation of the crude product by slow diffusion of Et_2O into a MeCN solution gave $[Cu(L^2)(ClO_4)]ClO_4 \cdot \frac{1}{2}H_2O$ (60% yield) as well shaped light blue prisms: m.p. 270 °C with decomposition. Elemental Analysis: *Anal.* Calc. for $C_{19}H_{21}Cl_2CuN_2O_{8.5}S_2$: C, 37.3; H, 3.5; N, 4.6; S, 10.5. Found: C, 37.5, H, 3.3, N, 4.6, S, 10.6%. FAB mass spectrum (3-noba matrix): *m/z* 502, 403; calc. for $[^{63}Cu(L^2)(ClO_4)]^+$ and $[^{63}Cu(L^2)]^+$ 502 and 403, respectively. Electronic spectrum (MeCN): $\lambda_{max} = 230$ ($\varepsilon_{max} = 45\,000$), 278 (29 100), 360 (4400), 630 nm (400 M^{-1} cm^{-1}).

3: Crystals of good quality were not obtained upon re-crystallisation (61% yield) (m.p. = 250°C with decomposition). Elemental Analysis: *Anal.* Calc. for $C_{18}H_{18}Cl_2CuN_2O_8S_3$: C, 34.8; H, 2.9; N, 4.5; S, 15.5. Found: C, 34.8; H, 2.8; N, 4.5; S, 15.4%. FAB mass spectrum (3-noba matrix): *m/z* 521, 421; calc. for $[^{63}Cu(L^3)(ClO_4)]^+$ and $[^{63}Cu(L^3)]^+$ 521 and 421, respectively. Electronic spectrum (MeCN): $\lambda_{max} = 230$ ($\lambda_{max} = 34\,540$), 278 (28 300), 355 (4000), 592 nm (250 M^{-1} cm^{-1}).

2.2. Synthesis of $[Cu(L^3)_2](PF_6)_2$ (**4**)

A mixture of L^3 (50 mg, 0.139 mmol) and $CuCl_2 \cdot 2H_2O$ (23.8 mg, 0.139 mmol) in $MeCN/H_2O$ (20 ml, 1:1 v/v) was refluxed under N_2 for 2 h. Addition of a large excess of NH_4PF_6 to the resulting solution afforded a brick red solid of $[Cu(L^3)_2](PF_6)_2$ (20 mg, 14% yield): m.p. 230 °C with decomposition. Elemental Analysis: *Anal.* Calc. for $C_{36}H_{36}CuF_{12}N_4P_2S_6$: C, 40.4; H, 3.4; N, 5.2; S, 18.0. Found: C, 40.4; H, 3.6; N, 5.7; S, 17.7%. FAB mass spectrum (3-noba matrix): *m/z* 421; calc. for $[^{63}Cu(L^3)]^+$ 421. Electronic spectrum (MeCN): $\lambda_{max} = 275$ ($\varepsilon_{max} = 10\,800$), 377 (3400), 467 (1100), 750 nm (140 M^{-1} cm^{-1}).

2.3. Synthesis of $[Cu(L^3)(Cl)(PPh_3)]$ (**5**)

A solution of L^3 (20 mg, 0.06 mmol) in CH_2Cl_2 (1.5 ml) was added to a suspension of $[CuCl(PPh_3)_3]$ (50 mg, 0.06 mmol) in EtOH (2 ml) maintained at room temperature under N_2. After filtration of the solution and about one hour, $[Cu(L^3)(Cl)(PPh_3)]$ (8.7 mg, 22.4% yield) was obtained as prism orange crystals: m.p. 270 °C with decomposition. Elemental Analysis: *Anal.* Calc. for $C_{36}H_{33}ClCuN_2PS_3$: C, 60.1; H, 4.6; N, 3.9; S, 13.4. Found: C, 60.3; H, 4.5; N, 3.8; S, 13.4%. FAB mass spectrum (3-noba matrix): *m/z* 421; calc. for $[^{63}Cu(L^3)]^+$ 421. ^{1}H-NMR (300 MHz, 298 K, CD_2Cl_2): δ_H 8.26 (d, 2H, $J = 7.8$ Hz), 7.76 (s, 2H), 7.71 (d, 2H, $J = 7.8$ Hz), 7.26–7.05 (m, 15H), 4.5 (s, 4H), 3.10 (m, 4H), 2.7 (m, 4H). ^{13}C-NMR (75.4 MHz, 298 K, CD_2Cl_2): δ_C 160.6, 142.9, 137.7, 134.1, 133.9, 129.2, 128.3, 128.2, 127.7, 126.2, 125.0, 38.3, 34.5, 33.4. Electronic spectrum (CH_2Cl_2): $\lambda_{max} = 273$ ($\varepsilon_{max} = 26\,000$), 427 nm (650 M^{-1} cm^{-1}).

2.4. Spectrophotometric titrations

In order to monitor complex formation between L^1–L^3 and Cu^{II}, 2 ml of the copper solution in MeCN or EtOH (4×10^{-4}–5×10^{-4} M) was placed in a 1 cm optical path quartz cell thermostated at 25 °C. A known amount of the ligand ($L/Cu^{II} = 0.2$–4) was added to the cell and the spectra were recorded soon after addition of the ligand to the copper solution.

2.5. Crystallography

Crystal data and refinement details of all structure determinations are summarised in Table 1. Only special features of the analyses are pointed out here. Single crystal data collections for $L^2 \cdot H_2O$ and $[Cu(L^1)(ClO_4)]ClO_4$ (**1**) were performed at room temperature on a CAD-4 diffractometer using ω scans. For $[Cu(L^2)(ClO_4)]ClO_4 \cdot \frac{1}{2}H_2O$ (**2**) and $[Cu(L^3)(Cl)(PPh_3)]$ (**5**), data were acquired at room temperature on a SMART CCD diffractometer (ω scans) and a Rigaku AFC5S diffractometer ($\omega-\theta$ scans), respectively. All data sets were corrected for Lorentz-polarisation effects and for absorption as specified in Table 1. The structures were solved by direct methods using the SHELXS program [24] followed by difference Fourier synthesis and refined by full matrix least-squares on F^2 [25]. All non-H atoms were refined anisotropically and H atoms were introduced at calculated positions and thereafter incorporated into a riding model with $U_{iso}(H) = 1.2U_{eq}(C)$. In $L^2 \cdot H_2O$, the carbon atoms C(18) and C(19) in the aliphatic portion of the ring between the two S-donors were found to be disordered. The disorder was modelled setting for each carbon atom the occupancy of the two disordered sites to 0.65 and 0.35, respectively. Appropriate restraints were applied to the bond lengths of the disordered portion of the macrocyclic ligand, both components being refined isotropically. The H atoms could not be included in the refinement model. The positions of the H atoms of the water molecule were seen in a difference Fourier map and were refined. For $[Cu(L^2)(ClO_4)]ClO_4 \cdot \frac{1}{2}H_2O$ (**2**), the space group cannot be uniquely determined from systematic absences being the *C*2/*m*, *C*2 and *Cm* space groups possible. The

Table 1
Summary of crystallographic data for $L^2 \cdot H_2O$, $[Cu(L^1)(ClO_4)]ClO_4$ (**1**), $[Cu(L^2)(ClO_4)]ClO_4 \cdot \frac{1}{2}H_2O$ (**2**), and $[Cu(L^3)(Cl)(PPh_3)]$ (**5**)

Compound	$L^2 \cdot H_2O$	$[Cu(L^1)(ClO_4)]ClO_4$ (**1**)	$[Cu(L^2)(ClO_4)]ClO_4 \cdot \frac{1}{2}H_2O$ (**2**)	$[Cu(L^3)(Cl)(PPh_3)]$ (**5**)
Formula	$C_{19}H_{22}N_2OS_2$	$C_{18}H_{18}Cl_2CuN_2O_9S_2$	$C_{19}H_{21}Cl_2CuN_2O_{8.5}S_2$	$C_{36}H_{33}ClCuN_2PS_3$
M	358.51	604.90	611.94	719.78
Crystal system	monoclinic	monoclinic	monoclinic	monoclinic
Space group	$P2_1/n$ (No. 14)	$P2_1/c$ (No. 14)	$C2/m$ (No. 12)	$P2_1/c$ (No. 14)
a (Å)	7.653(1)	9.063(3)	13.242(2)	9.915(2)
b (Å)	19.644(3)	11.872(3)	11.623(1)	33.468(2)
c (Å)	11.979(2)	20.658(10)	15.950(2)	10.374(2)
β (°)	90.72(1)	93.03(4)	98.32(1)	99.72(1)
V (Å^3)	1800.8(5)	2219.6(14)	2429.1(5)	3393.0(10)
Z	4	4	4	4
D_c (g cm^{-3})	1.322	1.810	1.673	1.409
μ (Mo Kα) (mm^{-1})	0.304	1.469	1.342	0.983
Unique reflection (R_{int})	3145 (0.023)	3890 (0.018)	2285 (0.036)	5996 (0.034)
Observed reflections [$I > 2\sigma(I)$]	1367	2669	1440	3490
Absorption correction	ψ-scans	ψ-scans	SADABS [23]	ψ-scans
T_{min}, T_{max}	0.94, 1.00	0.91, 1.00	0.81, 1.00	0.719, 0.813
R_1	0.0707	0.0385	0.0596	0.0511
wR_2 [all data]	0.2010	0.1049	0.1894	0.1189

refinement carried out in the space group $C2/m$ gives a model with atom C(18) of the aliphatic moiety disordered over two positions. The corresponding refinement in the non centrosymmetric space group $C2$ provides a model with no disorder in the aliphatic moiety, but absolutely not reliable interatomic distances and displacement parameters for all the ''mirror-related'' atoms of the phenanthroline moiety, due to strong correlation in the refinement procedure. Any attempt to solve the structure in the space group Cm failed. Therefore, we consider space group $C2/m$ as the most appropriate for describing the structure of (**2**).

In $[Cu(L^3)(Cl)(PPh_3)]$ (**5**), the carbon atoms C(15) and C(16) between the S-donors S(1) and S(3) in the aliphatic portion of the ring were found to be disordered. In this case, the disorder was modelled by a partial occupancy over two sites for each of the carbon atoms, converging with factors of 0.58 and 0.42. Both components bearing H atoms positioned geometrically were refined anisotropically with appropriate restraints imposed to the bond lengths of the disordered portion of the ligand.

2.6. Molecular mechanics calculations

MM calculations were performed using the Spartan 5.0 program [26] as previously described [21]. The calculated conformers have been examined using the Molekel 4.3 program [27].

3. Results and discussion

3.1. Ligands

We reported previously the synthesis of the ligands L^1–L^3 and the X-ray crystal structure of L^1 [17–21]. After many attempts, we have also been able to grow single crystals of $L^2 \cdot H_2O$ from a MeCN/Et_2O solution. The crystal structure confirms the nature of the compound and shows the presence of disorder in the aliphatic portion of the ring between S(1) and C(17) (Fig. 1), analogously to what was found for one of the two independent molecules in the asymmetric unit of $L^1 \cdot \frac{1}{2}H_2O$ [20]. Molecular mechanics (MM) calculations previously performed on both L^1 and L^3 [20] have now been extended to L^2, with the aim to understand the effect on the flexibility of the aliphatic chain on removing one donor atom. The eight most stable conformers cal-

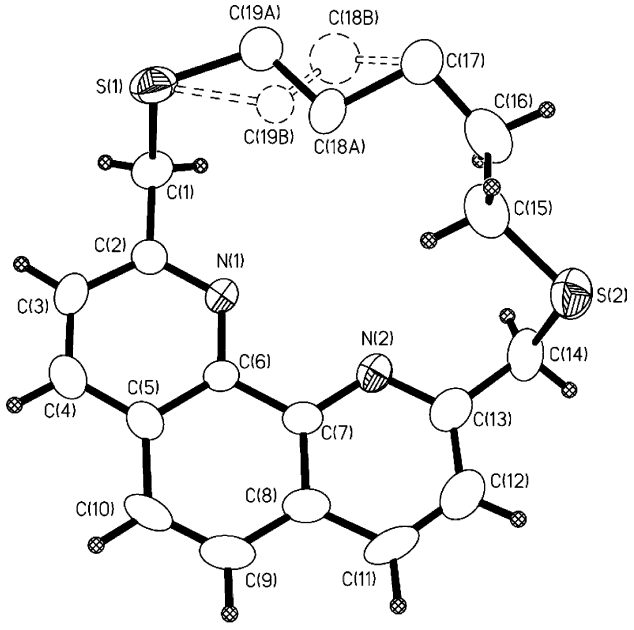

Fig. 1. ORTEP view of L^2 in the crystal structure of $L^2 \cdot \frac{1}{2}H_2O$. Atoms C(19A) and C(18A) comprise the major disordered component.

culated for L^2, which differ in energy by less than 12.5 kJ mol^{-1}, and their torsion angle have been deposited as ESI (Fig. S1, Table S1). Analogously to what was found for L^1 and L^3 [20], two features are common to all calculated conformations of L^2: (a) the aliphatic portion of the ring is folded over the plane of the phenanthroline unit, (b) the lone pairs on both S-donors adopt exodentate orientation pointing out of the macrocyclic cavity. Compared to L^1 and L^3 [20], the replacement of the O(S)-donor with a methylene group in L^2 causes a slight increase in the flexibility of the aliphatic chain connected to the phenanthroline unit. In fact, the torsion angles S(2)–C–C–X and X–C–C–S(1), which in the case of L^1 (X = O) and L^3 (X = S) assume *anti* arrangements in the most stable calculated conformers [20], can also assume *gauche* disposition in L^2 (X = CH_2). Furthermore, the torsion angles about the C–X bonds, which are one generally *gauche* and one *anti* in L^1 and L^3, can be both *anti* and both *gauche* for the most stable calculated conformers for L^2. A less regular trend is also observed for the torsion angles about the C–S(1) and C–S(2) bonds, which are generally *gauche* in the most stable calculated conformers of L^1 and L^3 [20]. Interestingly, the conformation adopted by the major disorder component in L^2 (Fig. 1) is very similar to the most stable calculated conformer, while that adopted by the minor disorder component is practically similar to that calculated for the sixth most stable conformer.

3.2. Complexation

The reaction of L^1–L^3 with Cu^{II} has been studied spectrophotometrically both in EtOH and in MeCN. Immediately upon mixing the reactants, a blue-green colour is observed (λ_{max} = 650 nm). In time, this colour disappears and solutions turn to yellow. This behaviour is observed for all three ligands in EtOH and MeCN, and for solutions having different L/Cu^{II} molar ratios (from 0.2 to 4). However, the blue-green colour persists for several hours if the L/Cu^{II} molar ratio is lower than 1.

In order to understand the stoichiometry of the Cu^{II} species responsible for the blue-green colour, due to their instability in the presence of excess ligands, we carried out fast spectrophotometric titrations of Cu^{II} with the ligands in EtOH or MeCN by recording the spectra immediately after mixing the reactants. The absorbance (370 nm)/molar ratio plots show a sharp inflection point at the 1:1 (L/Cu^{II}) molar ratio (Fig. 2) and thus indicate a quantitative formation of $[Cu(L)]^{2+}$ (L = L^1–L^3) complexes. It is interesting to observe that further addition of the ligands beyond the 1:1 L/Cu^{II} molar ratio led to a gradual small decrease in absorbance at 370 nm, according to the observed instability of the species $[Cu(L)]^{2+}$ in the presence of excess ligands; this effect is particularly evident in the case of L^2 (see Fig. 2). However, the transformation of the $[Cu(L)]^{2+}$ species is slow enough to allow confirmation of their 1:1 stoichiometry by continuous variations plots in EtOH under similar experimental conditions and to allow their isolation at the solid state.

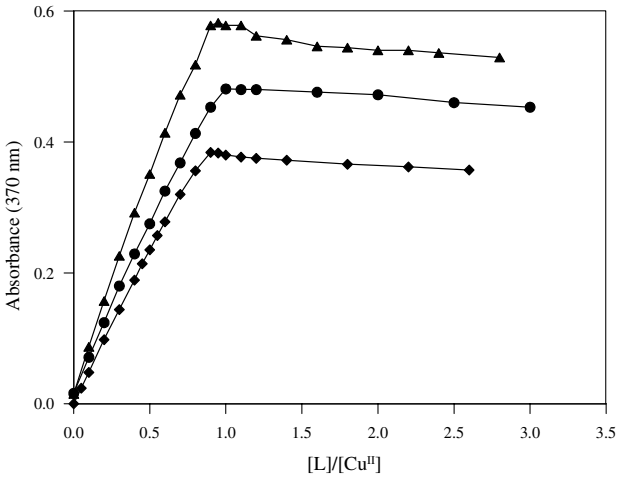

Fig. 2. Absorbance (370 nm) vs L/Cu^{II} molar ratio plots for EtOH solutions at 25 °C of Cu^{II} (2×10^{-4} M) and L^1 (◆) L^2 (▲) or L^3 (●) immediately after mixing the reactants.

In fact, whatever the Cu^{II}/L molar ratio used (1:1 or 1:2), the reaction between L^1–L^3 and $Cu(ClO_4)_2 \cdot 2H_2O$ in EtOH/CH_2Cl_2 always resulted in solid products containing the 1:1 complexes, as demonstrated by elemental analysis, FAB mass spectrometry (see Section 2), and X-ray structural analysis for $[Cu(L^1)(ClO_4)]ClO_4$ (**1**) and $[Cu(L^2)(ClO_4)]ClO_4 \cdot \frac{1}{2}H_2O$ (**2**). Several attempts were made to isolate 1:2 Cu^{II}/L complexes at the solid state using different starting copper(II) metal salts and solvents. Only from the reaction of L^3 with $CuCl_2 \cdot 2H_2O$, and after addition of excess of NH_4PF_6 to the reaction mixture, was the complex $[Cu(L^3)_2][PF_6]_2$ (**4**) separated as a red microcrystalline solid. Unfortunately, all attempts to grow good quality single crystals for this compound failed. The complexing ability of L^1–L^3 was also tested toward stoichiometric amounts of the Cu^{I} salt $[CuCl(PPh_3)_3]$ in an EtOH/CH_2Cl_2 mixture, and only in the case of L^3 was it possible to isolate the complex $[Cu(L^3)(Cl)(PPh_3)]$ (**5**), of which good quality crystals suitable for X-ray diffraction studies were grown by slow evaporation of the reaction mixture.

3.3. X-ray diffraction analysis

In **1** (Fig. 3, Table 2), L^1 acts as an N_2S_2O-donor, encapsulating the copper(II) ion within a cavity having a square-based pyramidal geometry with the equatorial positions occupied by the two N-donors of the phenanthroline moiety [Cu–N 1.969(3) and 1.964(3) Å] and by the two S-donors of the aliphatic linker [Cu–S 2.361(1)

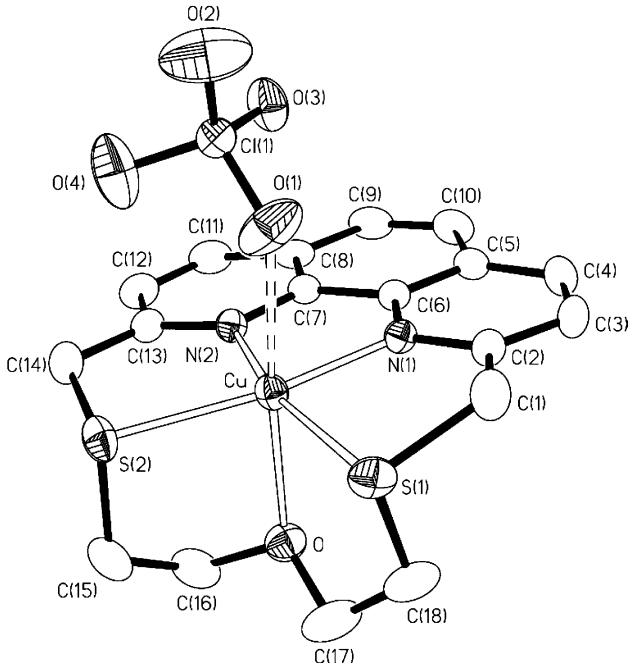

Fig. 3. ORTEP of the $[Cu(L^1)(ClO_4)]^+$ complex cation in **1** with the adopted numbering scheme. Displacement ellipsoids are drawn at 30% probability and hydrogen atoms are omitted for clarity.

and 2.364(1) Å], and the axial position occupied by the O-donor [Cu–O 2.304(3) Å]. The Cu^{II} ion lies in the plane defined by the atoms N(1), N(2), S(1), and S(2), and an overall *pseudo* octahedral coordination sphere is reached at the metal centre by interaction of a perchlorate ion acting as a monodentate ligand at the coordination site left free by the pentadentate macrocyclic ligand [Cu–O(1) 2.648(5) Å, O–Cu–O(1) 165.94(11)°]. L^1 therefore adopts a folded conformation typical for this type of macrocycles with the aliphatic chain of the ring tilted over the plane containing the phenanthroline unit. Interestingly, the L^1 donation to Cu^{II} is comparable with that of [15]aneN_2OS_2 observed in $[Cu([15]aneN_2OS_2)]^{2+}$: in this latter complex, the more flexible aliphatic macrocyclic ligand imposes a similar square-based pyramidal N_2S_2O environment at the metal centre with metal–donor atom distances (Cu–N 1.97, Cu–S 2.31, Cu–O 2.28 Å) very similar to those found in **1** [28].

Fig. 4 shows the structure of the complex cation $[Cu(L^2)(ClO_4)]^+$ in **2** obtained from the reaction of copper(II) perchlorate with L^2 in EtOH/CH_2Cl_2. Selected bond distances and angles are given in Table 2. The complex cation sits on a mirror plane and the Cu^{II} ion resides in a distorted square-based pyramidal $N_2S_2O_2$ environment with the basal positions occupied by the four donors of the macrocyclic ligand and the apical site occupied by a bidentate perchlorate group. The Cu–N and Cu–S bond lengths are comparable to those observed in $[Cu(L^1)]^{2+}$ and the metal centre is displaced

Table 2
Selected bond lengths (Å) and angles (°) for $[Cu(L^1)(ClO_4)]ClO_4$ (**1**), $[Cu(L^2)(ClO_4)]ClO_4 \cdot \frac{1}{2}H_2O$ (**2**) and $[Cu(L^3)(Cl)(PPh_3)]$ (**5**)[a]

	$[CuL^1(ClO_4)]ClO_4$ (**1**)	$[Cu(L^2)(ClO_4)]ClO_4 \cdot \frac{1}{2}H_2O$ (**2**)[b]	$[CuL^3(Cl)(PPh_3)]$ (**5**)
Cu–S(1)	2.361(1)	2.347(2)	
Cu–S(2)	2.364(1)		
Cu–N(1)	1.969(3)	1.956(5)	2.140(4)
Cu–N(2)	1.964(3)		2.120(4)
Cu–X(1)	2.304(3)	2.750(12)	2.226(2)
Cu–X(2)	2.648(5)		2.263(2)
N(1)–Cu–N(2)	82.48(13)		77.60(16)
N(1)–Cu–N(1^i)		83.0(3)	
N(1)–Cu–S(1)	82.82(10)	82.9(1)	
N(1)–Cu–S(2)	165.93(10)		
N(1)–Cu–S(1^i)		163.7(2)	
N(1)–Cu–X(1)	99.42(12)	112.7(2)	102.04(11)
N(1)–Cu–X(2)	82.09(14)	84.7(2)	118.21(12)
N(2)–Cu–S(1)	164.32(10)		
N(2)–Cu–S(2)	83.45(10)		
N(2)–Cu–X(1)	95.58(12)		117.88(12)
N(2)–Cu–X(2)	98.46(13)		115.21(11)
S(1)–Cu–S(2)	111.21(5)		
S(1)–Cu–S(1^i)		109.8(9)	
S(1)–Cu–X(1)	81.49(8)	108.4(2)	
S(1)–Cu–X(2)	84.86(10)	74.0(2)	
S(2)–Cu–X(1)	82.19(9)		
S(2)–Cu–X(2)	99.76(11)		
X(1)–Cu–X(2)	165.94(11)	42.4(4)	118.26(6)

No significant interactions between Cu^I and S-donors are present in **5**: Cu–S(1) 4.728(2), Cu–S(2) 4.689(2) Å.

[a] X(1) = O(**1**), O(5)ClO_3 (**2**), PPh_3 (**5**); X(2) = O(1)ClO_3 (**1**), O(5^i)ClO_3 (**2**), Cl (**5**).

[b] The complex cation $[Cu(L^2)(ClO_4)]^+$ in **2** lies across a mirror plane, $i = x, -y, z$.

0.140 Å out of the mean plane defined by the atoms N(1), N(1^i), S(1), and S(1^i) towards the ClO_4^- ligand.

The reaction of L^3 with $CuCl(PPh_3)_3$ in EtOH/CH_2Cl_2 afforded the complex $[Cu(L^3)(Cl)(PPh_3)]$ (**5**) (Fig. 5, Table 2). The Cu^I ion is coordinated by the nitrogen donors of L^3 [Cu–N 2.140(4), 2.120(4) Å], a PPh_3 unit [Cu–P 2.226(2) Å], and a chloride ligand [Cu–Cl 2.263(2) Å] to complete a distorted tetrahedral coordination sphere. The S-donors in the aliphatic chain of L^3 remain uncoordinated. The rigidity of the phenanthroline unit forces the angle N(1)–Cu–N(2) to assume a value of 77.60(16)°, thus allowing the P–Cu–Cl angle to open to the value of 118.26(6)°. The metal ion is located under the plane of the phenanthroline moiety with the formation of a five-membered chelate ring showing a pseudo-boat conformation. The dihedral angle between the plane of the phenanthroline moiety and the plane containing the atoms N(1), Cu, and N(2) is 21° as compared to values not greater than 8° observed for other Cu^I complexes with phenanthroline-based ligands (from a recent search of the Cambridge Crystallographic Database) [29].

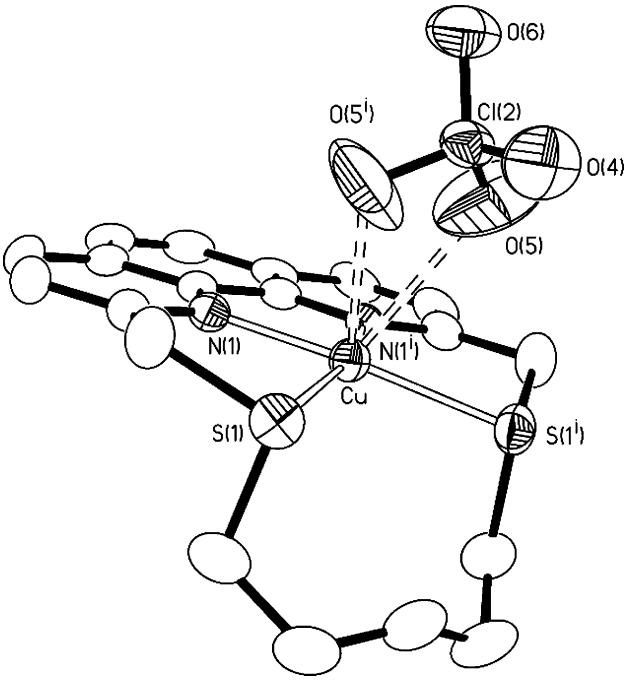

Fig. 4. ORTEP of the $[Cu(L^2)(ClO_4)]^+$ complex cation in **2** with the adopted numbering scheme. Displacement ellipsoids are drawn at 30% probability and hydrogen atoms are omitted for clarity.

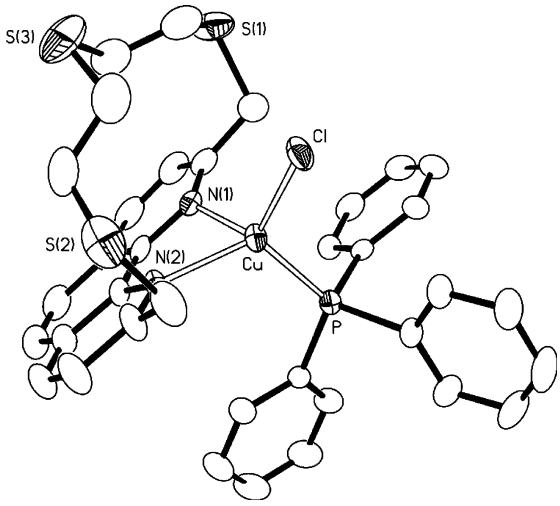

Fig. 5. ORTEP of $[Cu(L^3)(Cl)(PPh_3)]$ (**5**) with the adopted numbering scheme. Displacement ellipsoids are drawn at 30% probability and hydrogen atoms are omitted for clarity.

3.4. Spectral properties of complexes *1–4*

The electronic spectral features of complexes **1**, **2**, and **3** in MeCN solution are very similar (Table 3). The intense band observed at 278 nm (ε = 28 300–29 600 $M^{-1}\,cm^{-1}$) and the one at about 360 nm (ε = 4000–4400 $M^{-1}\,cm^{-1}$) can be assigned to the phenanthroline $\pi \rightarrow \pi^*$ and to a $S(\sigma) \rightarrow Cu^{II}$ ligand-to-metal (LMCT) charge-transfer transition, respectively [16,30,31].

The blue band at about 600 nm can be attributed to a d–d electronic transition and the fairly high molar extinction coefficient values observed (ε = 250–400 $M^{-1}\,cm^{-1}$, see Table 3) can be justified by the low symmetry of the complexes. However, it is opportune to remember that a band at about 600 nm with a much higher molar extinction coefficient (ε = 2000–6000 $M^{-1}\,cm^{-1}$)[1] is typical of the electronic spectra of Type-1 blue copper proteins and was assigned to a $S_{Cys}(\pi) \rightarrow Cu^{II}$ transition [16,30,31]. Therefore, a contribution of a $S(\pi) \rightarrow Cu^{II}$ LMCT transition to the band at

Table 3
Spectral and electrochemical data for the isolated Cu^{II} complexes **1–4** in MeCN solution[a]

Complex	Electronic spectra λ/nm (ε/$M^{-1}cm^{-1}$)	EPR spectra[b]		$E_{1/2}$ (V)
		Powder	Frozen MeCN solution[c]	
$[Cu(L^1)(ClO_4)]ClO_4$(**1**)	278 (29 600) 361 (4400) 639 (400)	$g_\parallel$ 2.181 $g_\perp$ 2.049	$g_\parallel$ 2.196 $g_\perp$ 2.038 $A_\parallel$ 170.2	+0.33
$[Cu(L^2)(ClO_4)]ClO_4 \cdot \frac{1}{2}H_2O$ (**2**)	278 (29 100) 360 (4400) 630 (400)	$g_\parallel$ 2.168 $g_\perp$ 2.054	$g_\parallel$ 2.182 $g_\perp$ 2.033 $A_\parallel$ 171.7	+0.33
$[Cu(L^3)](ClO_4)_2$ (**3**)	278 (28 300) 355 (4000) 592 (250)	$g_\parallel$ 2.151 $g_\perp$ 2.042	$g_\parallel$ 2.191 $g_\perp$ 2.036 $A_\parallel$ 168.6	+0.42
$[Cu(L^3)_2](PF_6)_2$ (**4**)	275 (10 800) 377 (3400) 467sh (1100) 750 (140)	$g_\parallel$ 2.169 $g_\perp$ 2.065 $A_\parallel$ 173	$g_\parallel$ 2.175 $g_\perp$ 2.040 $A_\parallel$ 180	+0.44

[a] All measurements were carried out in MeCN rather than in EtOH solutions for solubility reasons.
[b] $A_\parallel$ values are in units of $10^{-4}\,cm^{-1}$.
[c] MeCN solutions obtained by mixing L^1, L^2 or L^3 and $Cu(ClO_4) \cdot 2H_2O$ in 1:1 molar ratio; in the case of **4**, the solution was prepared by dissolving the solid complex in MeCN.

about 600 nm observed for **1**–**3** in MeCN might also be hypothesised.

The UV–Vis spectrum $[Cu(L^3)_2](PF_6)_2$ (**4**) in MeCN is quite different from those recorded for **1**–**3**, in fact besides a d–d electronic transition at 750 nm ($\varepsilon = 140\ M^{-1}\ cm^{-1}$) a shoulder at 467 nm ($\varepsilon = 1100\ M^{-1}\ cm^{-1}$) is also present.

The X-band EPR spectra of **1**, **2**, **3**, and **4** were recorded as solid powders and as frozen (77 K) MeCN glasses (Table 3). The EPR spectra of **1**, **2**, and **3** measured as powder are clearly axial and no hyperfine coupling to the metal centre is observed [32–34]. In the case of **4**, the axial EPR spectrum shows three of the four expected hyperfine signals in the parallel region, with the fourth being hidden under the $g_\perp$ region lines (Fig. 6). Furthermore, for **4**, a superhyperfine coupling can be observed in the perpendicular region of the spectrum, which is consistent with the presence of not less than three N-donors in the coordination sphere of the metal centre. Although very useful, this information does not allow to fully elucidate the coordination sphere around the metal centre in **4**. Interestingly, the $g_\parallel$-value decreases on passing from **1** to **3**, which reflects the substitution of an O-donor with a S-donor in the coordination sphere around the metal centre [35]. The EPR spectra measured as frozen MeCN glasses show isotropic signals with g_{iso} values of 2.093, 2.092, and 2.077 for **1**, **2**, and **3**, respectively. In the case of **4**, the EPR spectrum as frozen MeCN glass is very similar to that recorded as powder (Table 3). In order to better understand the nature of complexes **1**, **2**, and **3** in MeCN solution, the EPR spectra for mixtures of L^1, L^2 or L^3 and $Cu(ClO_4)_2$ in molar ratio 1:1 were recorded. For all three cases, the recorded EPR spectrum is typical of mononuclear Cu^{II} complexes with a tetragonal or square-based pyramidal coordination geometry at the metal centre (Table 3). Only three of the four expected hyperfine lines are observed in the parallel region; for **1** and **2**, and less marked for **3**, a superhyperfine coupling is also present in the perpendicular region, which accounts for the presence of two N atoms in **1** and at least three N atoms in **2** and **3** coordinated to the metal centre, probably due to the coordination of MeCN molecules.

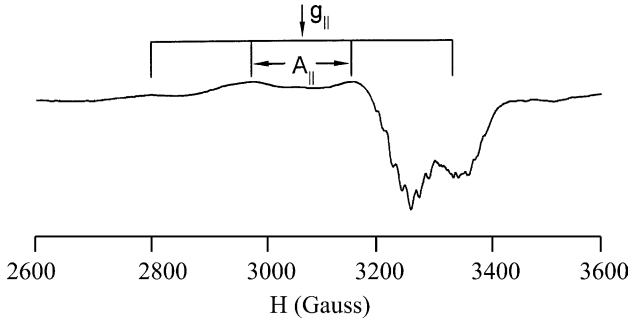

Fig. 6. X-band EPR spectra recorded at the solid state for $[Cu(L^3)_2](PF_6)_2$ (**4**). $A_\parallel$ hyperfine splitting and $g_\parallel$ value are shown. Superhyperfine resonance lines are observed (see text).

The $g_\parallel$- and $A_\parallel$-values recorded for **1**, **2**, and **3** as frozen MeCN glasses can be compared with those recorded as frozen $EtOH/H_2O$ glasses for Cu^{II} complexes with aliphatic N_2S_2-donor macrocycles with a distorted square-planar coordination geometry at the metal centre: i.e., *cis*-[12]aneN_2S_2 ($g_\parallel = 2.174$, $A_\parallel = 152$), *cis*-[14]aneN_2S_2 ($g_\parallel = 2.145$, $A_\parallel = 170$), and *cis*-[16]aneN_2S_2 ($g_\parallel = 2.172$, $A_\parallel = 151$) [16].

In any case, these EPR parameters are significantly different from those reported for Type-1 blue copper proteins ($g_\parallel = 2.21$–2.29, $A_\parallel = 35$–63) [1], thus suggesting a higher delocalisation for the unpaired d-electron in the Cu^{II}-macrocyclic systems including those reported here. In fact, the structures of native blue copper proteins typically show a much longer $Cu–S_{Met}$ bond distance than that shown by $Cu–S_{Cys}$, thus creating a peculiar tetrahedral distorted coordination geometry around the metal centre.

3.5. Cyclic voltammetry

Cyclic voltammetry of $[Cu(L^1)(ClO_4)]ClO_4$ (**1**), $[Cu(L^2)(ClO_4)]ClO_4 \cdot \frac{1}{2}H_2O$ (**2**), $[Cu(L^3)](ClO_4)_2$ (**3**) and $[Cu(L^3)_2](PF_6)_2$ (**4**) at platinum electrodes in MeCN shows for each of them a quasi-reversible one-electron (coulometrically tested) reduction at $E_{1/2}$-values (vs Ag/AgCl) of +0.33 ($E_{pa} - E_{pc} = 90$), +0.33 ($E_{pa} - E_{pc} = 90$), +0.42 ($E_{pa} - E_{pc} = 70$), and +0.44 V ($E_{pa} - E_{pc} = 100$ mV) for **1**, **2**, **3**, and **4**, respectively, that can be assigned to the Cu^{II}/Cu^{I} couple (Table 3).

Despite the different coordination environment at the metal centre in **1** and **2**, the Cu^{II}/Cu^{I} redox potentials for these two complexes are the same. The $E_{1/2}$-value recorded for **3**, instead, is significantly higher than those recorded for **1** and **2**, according to the increased number of coordinated S-donors in **3** that stabilises the metal centre in its reduced Cu^{I} form [14]. An increase in the Cu^{II}/Cu^{I} redox potential has also been observed for complexes with aliphatic macrocycles on passing from a N_4- to a N_2S_2-, and to a S_4-donor set [14]. The redox potential recorded for **2** is considerably higher than the $E_{1/2}$-values recorded in MeCN for Cu^{II} complexes with the aliphatic N_2S_2-donor macrocycles *cis*-[12]aneN_2S_2 ($E_{1/2} = 0.164$ V vs SHE), *cis*-[14]aneN_2S_2 ($E_{1/2} = 0.012$ V vs SHE), and *cis*-[16]aneN_2S_2 ($E_{1/2} = 0.368$ V vs SHE) [16], presumably due to the π-acceptor properties of the phenanthroline sub-unit, which stabilise the reduced Cu^{I} form. However, the $E_{1/2}$-value for **2** falls in the range 0.184–0.680 V (vs SHE in water solution) observed for the $E°$ of a series of Type-1 blue-copper proteins having an N_2S_2 trigonal pyramidal environment at the metal centre [6]. In the case of **1**, the value of $E_{1/2}$ is out of the range 0.285–0.310 V (vs SHE in water solution) generally reported for the $E°$ of Type-1

azurin proteins characterised by an N_2S_2O trigonal bipyramidal environment at the metal centre [6]. The $E_{1/2}$-value recorded for **4** and assigned to a Cu^{II}/Cu^{I} reduction process is very close to that of +0.603 (vs SHE in water solution) recorded for $[Cu(2,9\text{-dmphen})_2]^{2+}$ (2,9-dmphen = 2,9-dimethylphenanthroline) [36]. The mono-electron reduction of **4** was also monitored by UV–Vis spectroscopy. The in situ electrochemical reduction of $[Cu(L^3)_2](PF_6)_2$ (**4**) was carried out in MeCN (0.1 M $NBu^n_4BF_4$) at 298 K. The reduction proceeds with increasing of the band at 467 nm and a decreasing of the band at 750 nm (see above) recorded for the starting solution of **4**.

4. Conclusions

The coordination chemistry towards Cu^{II} of L^1, L^2, and L^3, having, respectively, N_2S_2O-, N_2S_2-, and N_2S_3-donor sets, and a phenanthroline sub-unit within the macrocyclic framework, has been studied. All three ligands form 1:1 Cu^{II}/L complexes both in solution (MeCN and EtOH) and in the solid state. X-ray diffraction analysis shows that the metal centre encapsulated within the macrocyclic ligands in a distorted square-based pyramidal or *pseudo*-octahedral coordination geometry, due to the interaction with also counteranion molecules. The ligands L^1 and L^2 have the right donor set to mimic the coordination environment of Type-1 blue copper proteins. However, the corresponding 1:1 CuN_2S_2O and CuN_2S_2 complexes tend to have square-based geometries in solution and in the solid state, because of the interaction with solvents and counter-anions, and because of the rigidity imposed by the phenanthroline framework to the cyclic systems.

Despite this, 1:1 Cu^{II} complexes with L^1 and L^2 show quasi-reversible redox potentials comparable to those observed for blue copper proteins. Due to its π-acceptor properties, the phenanthroline moiety certainly plays an important role in stabilising the metal centre in its Cu^{I} oxidation form. Because of the square-based nature of the Cu^{II} complexes with L^1 and L^2, the recorded hyperfine splitting constant ($A_{\|}$) is comparable to that observed for complexes with aliphatic N_xS_{4-x}-donating macrocycles, but different from that observed for blue copper proteins.

So far, the proposed models for blue copper proteins which comprise macrocyclic ligands have been somehow successful in reproducing the coordination environment around the metal; however, a single Cu^{II} complex with macrocyclic ligands, which shows redox, electronic, and EPR spectral properties reasonably similar to those of the native proteins, is still not available. The choice of macrocyclic ligands containing hetero-aromatic sub-units seems promising but it must be very well weighed so as to reach an appropriate balance between the donor properties and the flexibility of the aromatic fragments considered.

Acknowledgements

We thank the Ministero Italiano dell'Università e della Ricerca Scientifica e Tecnologica (MIUR) for financial support (FIRB project RBAU01HFNS). L.E. and V.M. thank the financial assistance of the Spanish Government provided by the Project BQU2000-0233.

Appendix A. Supplementary data

Full crystallographic data for the reported compounds have been deposited with the Cambridge Crystallographic Data Centre, CCDC No. 213075-213078. Copy may be obtained free of charge from The director, CCDC, 12 Union Road, Cambridge CB2 1Ez, UK (fax: +44-1223-336-033; e-mail: deposit@ccdc.cam.ac.uk or http://www.ccdc.cam.ac.uk). The eight most stable conformers calculated for L^2 and their torsion angles are also available as supplementary material (Fig. S1, Table S1). Supplementary data associated with this article can be found, in the online version at doi:10.1016/j.ica.2005.01.014.

References

[1] A.G. Sykes, Adv. Inorg. Chem. 36 (1991) 377, and references therein.
[2] P.M. Colman, H.C. Freeman, J.M. Guss, M. Murata, V.A. Norris, J.A.M. Ramshaw, M.P. Ventakappa, Nature 272 (1978) 319.
[3] J.M. Guss, E.A. Merritt, R.P. Phizackerley, B. Hedman, M. Murata, R.O. Hodgson, H.C. Freeman, Science 241 (1988) 806.
[4] E.T. Adman, S. Turley, R. Branson, K. Petratos, D. Banner, D. Tsernoglov, D. Beppo, H. Watanabe, J. Biol. Chem. 264 (1989) 87.
[5] F.N. Baker, J. Mol. Biol. 203 (1988) 1071.
[6] H.B. Gray, B.G. Malmström, R.J.P. Williams, J. Biol. Inorg. Chem. 5 (2000) 551.
[7] K.B. Yatsimirskii, V.V. Pavlishchuk, J. Coord. Chem. 37 (1996) 341, and references therein.
[8] P.L. Holland, W.B. Tolman, J. Am. Chem. Soc. 122 (2000) 6331.
[9] M. Vaidyanathan, R. Balamurugan, U. Sivagnanam, M. Palaniandar, J. Chem. Soc., Dalton Trans. (2001) 3498.
[10] H.C. Freeman, in: J.P. Laurent (Ed.), Coordination Chemistry, vol. 21, Pergamon, Oxford, 1981, p. 29.
[11] O. Farver, I. Pecht, Coord. Chem. Rev. 94 (1989) 17, and references therein.
[12] A.J. Blake, M. Schröder, Adv. Inorg. Chem. 35 (1990) 1, and references therein.
[13] G. Reid, M. Schröder, Chem. Soc. Rev. 19 (1990) 239.
[14] V. McKee, Adv. Inorg. Chem. 40 (1993) 323.
[15] K.K. Nanda, A.W. Addison, R.J. Butcher, M.R. McDevitt, T. Nageswara Rao, E. Sinn, Inorg. Chem. 36 (1997) 134.
[16] L. Siegfried, T.A. Kaden, Helv. Chim. Acta 67 (1984) 29.

[17] A.J. Blake, F. Demartin, F.A. Devillanova, A. Garau, F. Isaia, V. Lippolis, M. Schröder, G. Verani, J. Chem. Soc., Dalton Trans. (1996) 3705.
[18] F. Contu, F. Demartin, F.A. Devillanova, A. Garau, F. Isaia, V. Lippolis, A. Salis, G. Verani, J. Chem. Soc., Dalton Trans. (1997) 4401.
[19] A.J. Blake, J. Casabò, F.A. Devillanova, L. Escriche, A. Garau, F. Isaia, V. Lippolis, R. Kivekas, V. Muns, M. Schröder, R. Sillanpää, G. Verani, J. Chem. Soc., Dalton Trans. (1999) 1085.
[20] M. Arca, A.J. Blake, J. Casabò, F. Demartin, F.A. Devillanova, A. Garau, F. Isaia, V. Lippolis, R. Kivekas, V. Muns, M. Schröder, G. Verani, J. Chem. Soc., Dalton Trans. (2001) 1180.
[21] M.C. Aragoni, M. Arca, F. Demartin, F.A. Devillanova, A. Garau, F. Isaia, V. Lippolis, F. Jalali, U. Papke, M. Shamsipur, L. Tei, A. Yari, G. Verani, Inorg. Chem. 40 (2002) 323.
[22] L.-Y. Chunng, E.C. Constable, M.S. Khan, J. Lewis, P.R. Raithby, M.D. Vargas, J. Chem. Soc., Chem. Comm. (1984) 1425.
[23] SADABS Area-Detector Absorption Correction Program, Bruker AXS, Inc., Madison, WI, USA, 2000.
[24] G.M. Sheldrick, SHELXS 97, Acta Crystallogr., Sect A 46 (1990) 467.
[25] G.M. Sheldrick, SHELXL 97, Universität Göttingen, 1997.
[26] Spartan Version 5.0, Wavefunction Inc., 18401 Von Karman Ave., Ste. 370, Irvine, CA 92612, USA.
[27] S. Potmann, H.P. Luthi, Chimia 54 (2000) 766.
[28] F. Arnaud-Neu, M.J. Shwing-Weill, R. Louis, R. Weiss, Inorg. Chem. 18 (1979) 2956.
[29] (a) F.H. Allen, O. Kennard, Chem. Des. Autom. News 8 (1) (1993) 1;
(b) F.H. Allen, O. Kennard, Chem. Des. Autom. News 8 (1) (1993) 31, Cambridge Structural database Version 5.23, released April 2002.
[30] J.V. Dagdigian, V. McKee, C.A. Reed, Inorg. Chem. 21 (1982) 1332.
[31] V.M. Miskowski, J.A. Thich, R. Solomon, H.J. Schugar, J. Am. Chem. Soc. 98 (1976) 8344.
[32] I.M. Procter, B.J. Hathaway, D.E. Billing, R. Dudley, P. Nicholls, J. Chem. Soc. A (1969) 1192.
[33] D.E. Billing, R. Dudley, B.J. Hathaway, A.A.G. Tomlinson, J. Chem. Soc. A (1971) 691.
[34] A.W. Addison, E. Sinn, Inorg. Chem. 22 (1983) 1225.
[35] J. Peisach, W.E. Blumberg, Arch. Biochem. Biophys. 165 (1974) 691.
[36] B.J. Hathaway, in: G. Wilkinson (Ed.), Comprehensive Coordination Chemistry, vol. 5, 1987, p. 533.